Electrocatalysis (2013) 4:203–211
DOI 10.1007/s12678-013-0129-2

Reduction of Nitrate Ions at Rh-Modified Ni Foam Electrodes

Enrico Verlato · Sandro Cattarin · Nicola Comisso · Luca Mattarozzi · Marco Musiani · Lourdes Vázquez-Gómez

Published online: 13 April 2013

Abstract Commercial Ni foams were modified by spontaneous deposition of Rh nanoparticles, achieved by immersion of foam samples in acid, deaerated Na_3RhCl_6 solutions, at open circuit. The surface area of the Rh deposits was estimated, for different Rh loadings, by measuring the H adsorption/desorption charge. The surface area per unit Rh mass was found to exceed 50 $m^2\ g^{-1}$, for loading values below 2 mg cm^{-3}. The Rh-modified Ni foam electrodes were used as cathodes for the reduction of nitrate ions, and showed good catalytic activity, increasing with the Rh loading in a sublinear way; thus, the mass activity of the electrodes was higher at low loading. Prolonged electrolyses showed that the Rh-modified Ni foam electrodes underwent only moderate poisoning. Ion chromatography was used to assess the reaction products: irrespective of the Rh loading, ammonia was the main product, and nitrite accounted only for a few percent of the reduced nitrate. The beneficial effect of forcing a solution flow through the foam pores on the nitrate reduction current was shown.

Keywords 3D cathode · Degradation of pollutants · Electrocatalysis · Porous electrode · Spontaneous deposition

Introduction

The possibility to attain a large electrochemically active surface area per unit volume by using porous 3D electrodes was realized several decades ago [1–5] and this stimulated the development of electrodes with a number of different geometries, e.g., packed or fluidized particle beds, meshes, felts, foams, etc. Many metal foams, consisting of either pure metals or alloys, with a wide range of pore sizes and void volume fractions, are commercially available. With an appropriate choice of their characteristics, they may fulfill the requirements for effective operation as 3D electrodes in different electrochemical processes. Their large surface area may be entirely active if an even potential distribution and an efficient mass transfer are achieved. When used under forced electrolyte flow conditions, metal foam electrodes may ensure appropriate residence times of the reactants and promote turbulent flow with low pressure drop across the reactors [3, 6]. As compared with reticulated vitreous carbon, they are markedly less brittle.

Porous 3D electrodes have been employed in processes relevant to environmental electrochemistry, for example, removal of heavy metal ions from polluted waters [7–9] and degradation of complex organic molecules [10]. Metal recovery is not especially demanding in terms of cathode materials, as the electrodeposition of (noble) metals does not require a specific catalytic activity. Thus, the key issue is ensuring an effective mass transfer of the metal ions, generally present in solution at low concentrations, by using a forced electrolyte flow, in either flow-through or flow-by electrochemical reactors. Instead, the effective removal of some pollutants may require the use of appropriate electrocatalysts, often based on noble metals [6, 11, 12], to achieve a satisfactory reaction rate and selectivity. Therefore, surface modification of metal foams is an interesting strategy to enhance their catalytic activity towards specific substrates.

Noble metal-modified Ni foams have been studied by various groups, with the aim of producing electrodes for water electrolysers, fuel cells, hydrogen storage, or degradation of pollutants. Noble metal nuclei or thin layers were formed onto the foam substrates by either electrodeposition [13–18] or spontaneous deposition [19–26] taking place, at

This paper is dedicated to Prof. Achille De Battisti, on the occasion of his retirement.

E. Verlato · S. Cattarin · N. Comisso · L. Mattarozzi · M. Musiani (✉) · L. Vázquez-Gómez
IENI CNR, Corso Stati Uniti 4,
35127 Padua, Italy
e-mail: m.musiani@ieni.cnr.it

open circuit, through Ni-noble metal exchange reactions. The present paper reports on the preparation and characterization of Rh-modified Ni foam electrodes by spontaneous deposition and on their use as electrocatalysts for a process of potential interest in environmental electrochemistry: the reduction of nitrate and nitrite ions [27–36]. Rh has been reported to be the most active noble metal cathode for nitrate reduction in acid medium [29, 30], and its marked activity in basic medium has been also described [32, 34]. Ni cathodes were found to reduce nitrate to mixtures of products containing significant amounts of N_2, though with low conversion rate and low current efficiency [27]. Therefore, Ni modification with Rh nanodeposits is expected to create a large number of active catalytic sites by using only small amounts of noble metal, thus circumventing the problems associated with the high cost of Rh, which prevents its use as bulk material in practical applications. Our group recently reported on the preparation of Rh-modified Ni foams and on their use in the catalytic partial oxidation of CH_4-H_2 mixtures [37]; in the present paper, we describe how the Rh surface area per unit mass could be increased, as compared to the values reported in [37] by using different spontaneous deposition conditions.

Experimental

Preparation and Characterization of Rh-Modified Ni Foam Electrodes

Rh-modified Ni foam electrodes (henceforth denoted Rh-Ni) were produced, with procedures similar to those described in [37], using as substrates Ni foam samples cut from grade 50 INCOFOAM^{TM} sheets 0.17 cm thick, with apparent density 0.22 g cm^{-3}, corresponding to a void volume fraction of 0.975. The Ni foam samples were either $0.5\times0.5\times0.17$ cm or $1.0\times1.0\times0.17$ cm parallelepipeds (volumes 0.0425 or 0.17 cm^3, respectively). Before use, they were washed with acetone, then dichloromethane, dried in an air stream, etched in 2 M HCl at 60 °C for 15 min, and rinsed with water in an ultrasonic bath. After such a treatment, the Ni foam specific surface area (a_{Ni}, defined as the true surface area of 1 cm^3 volume of Ni foam) was in the range 270 to 300 cm^{-1} [25].

Rh deposition was performed by immersing the Ni foam samples, at open circuit, in deaerated solutions containing 4×10^{-4} M or 10^{-3} M Na_3RhCl_6, 1 M NaCl and HCl to adjust the pH at 2.0, kept at 25 °C with a thermostat. Since the formation kinetics of chloro-complexes of Rh is known to be slow [38], and their speciation may evolve during several days, solution aging had to be controlled in order to enhance the reproducibility of the deposition process. Na_3RhCl_6 solutions were normally used after aging for 2 days at 60 °C and at least 1 week at room temperature, after their preparation. The duration of the spontaneous deposition reaction (t_{SD}) was varied between 15 and 180 min. The amount of Rh deposited onto Ni was estimated by measuring the decrease in the Rh complexes concentration caused by each experiment, using ion chromatography [37].

Rh-Ni samples prepared with different combinations of t_{SD} and $[Na_3RhCl_6]$ values, resulting in different noble metal loadings (L_{Rh}; units, milligrams of Rh in a 1 cm^3 foam volume), were submitted to cyclic voltammetry to estimate their H adsorption/desorption charge, and hence the Rh surface area [39], by comparison with a carefully polished Rh disk electrode with a 0.0078-cm^2 geometric surface area, assumed to be identical to its true surface area. Electrical contact was made by passing a 0.5-mm Ni wire through a 0.5-mm diameter hole drilled in the Ni parallelepiped ahead of Rh deposition and twisting it firmly. The voltammetric experiments were performed in a two-compartment cell; the modified foam, used as working electrode, and a Pt wire counter electrode (ca. 10 cm^2 geometric area) were placed in the main compartment; an Hg|HgO|1 M KOH reference electrode was placed in the lateral compartment connected to the main one through a Luggin capillary. All potentials are referred to this reference electrode. Voltammetries were performed in 1 M KOH with a 50-mV s^{-1} scan rate. The voltammograms shown below correspond to a stabilized behavior.

The electrochemical equipment used in voltammetric experiments consisted of an Autolab PGSTAT 302N. Na_3RhCl_6 solutions were analyzed with a Metrohm 850 Professional IC liquid chromatographer equipped with a Metrohm 887 UV–Visible detector and a METROSEP A SUPP 15-50 anionic column. SEM images and EDS analyses were obtained with a Zeiss ∑IGMA instrument, equipped with a field emission gun, operating in high vacuum condition at an accelerating voltage variable from 5 to 30 keV, depending on the observation needs.

Nitrate (and Nitrite) Reduction

Nitrate (and nitrite) reduction was studied by cyclic voltammetry (using the cell described above and 0.1 M $NaNO_3$, 1 M NaOH solutions) and by prolonged potentiostatic electrolyses. The latter were performed in a two-compartment cell with working and reference electrodes in a compartment, containing 50 cm^3 of a 1-M NaOH, 0.1-M $NaNO_3$ solution, stirred with a magnetic bar, and a Ni wire counter electrode in the other compartment, containing 1 M NaOH (NaOH was preferred to KOH because, with our ion

chromatography procedure, NH_4^+ was more easily separated from Na^+ than from K^+). The compartments were separated by a Nafion™ 117 membrane; both were purged with nitrogen before the electrolyses. Electrolyses were performed at E=−1.20 V vs. Hg|HgO, using 0.17 cm^3 Rh-Ni working electrodes with different Rh loadings. An unmodified Ni foam electrode was also studied for comparison, under the same conditions. Experiments were run for the durations necessary to transfer a 2,000-C reduction charge, which would correspond to the conversion of about one half of the nitrate initially present, under the assumption of eight electrons per nitrate ion (reduction to NH_3) and 100 % efficiency. Solution samples (0.5 cm^3 each) were withdrawn every 500 C and analyzed by ion chromatography, using standard methods for the determination of NO_2^-, NO_3^-, NH_3, and NH_2OH [36]. Gaseous products were not analyzed.

Some nitrate reduction experiments were performed by forcing an electrolyte flow through Rh-Ni foams. A commercial two-electrode Micro Flow Cell, manufactured by ElectroCell A/S, Vennelystvej 1, DK 6880 Tarm, Denmark, with anode and cathode compartments separated by a Nafion™ 117 membrane, was used. Such a cell did not comprise a reference electrode. A compartment was filled with a 1-M KOH, 0.1-M $NaNO_3$ solution and contained a Rh-Ni 1.0×1.0×0.17 cm parallelepiped, placed with the 1.0×1.0-cm faces parallel to the membrane; one of these faces was in contact with the membrane, the other with a Ni sheet, to allow electrical contact. The electrolyte flow was perpendicular to the 1.0×0.17-cm faces of the foam and to the current flow (flow-by configuration). A NE-300 Programmable Syringe Pump, manufactured by Pump Systems Inc., allowed to control the electrolyte flow between 0 and 20 cm^3 min^{-1}, corresponding to linear flow rates up to ca. 2 cm s^{-1}. The other compartment was filled with a 0.2-M $K_3[Fe(CN)_6]$, 0.2-M $K_4[Fe(CN)_6]$, 1-M KOH solution in contact with a Pt sheet (10 cm^2 geometric area); this solution was not flowing during individual experiments but was renewed before each test. All solutions were deaerated and thermostated at 25 °C. In different experiments, the total cell voltage (ΔV_{cell}) was either maintained constant or varied linearly with time, at a 10-mV s^{-1} scan rate.

Results and Discussion

Preparation and Characterization of Rh-Modified Ni Foams

Solutions containing Na_3RhCl_6 at two different concentrations (4×10^{-4} and 10^{-3} M), 1 M NaCl and the HCl necessary to adjust the pH at 2.0, were used for the modification of Ni foams with Rh deposits. These solutions contained different chloro-complexes of Rh, mainly $RhCl_6^{3-}$, $RhCl_5(H_2O)^{2-}$, and $RhCl_4(H_2O)_2^{2-}$ [38], which reacted with Ni in metal exchange reactions:

$$3Ni + 2RhCl_6^{3-} \rightarrow 3Ni^{2+} + 2Rh + 12Cl^- \quad (1)$$

$$3Ni + 2RhCl_5(H_2O)^{2-} \rightarrow 3Ni^{2+} + 2Rh + 10Cl^- + 2H_2O \quad (2)$$

$$3Ni + 2RhCl_4(H_2O)_2^- \rightarrow 3Ni^{2+} + 2Rh + 8Cl^- + 4H_2O \quad (3)$$

The Rh loading of foam samples (L_{Rh}) was estimated by measuring the decrease in the concentration of Rh ions caused by deposition experiments, assuming that metallic Rh deposits accounted for all the ions consumed. SEM-EDS analyses showed that the walls of both the outer and the inner cells of the foam bore comparable Rh deposits. SEM images of Rh-Ni foam samples with similar Rh loading, prepared in 10^{-3} and 4×10^{-4} M Na_3RhCl_6 solutions, respectively, are compared in Fig. 1. The morphology of the deposits was significantly different: a larger surface density of tinier particles was present on the sample prepared, at a higher metal exchange rate, in the more concentrated solution.

In order to measure the surface area of the Rh deposits, Rh-modified Ni foam samples were submitted to cyclic voltammetry in 1 M KOH, using an anodic limit, E_A=-0.4 V, which did not cause significant Rh oxidation. Figure 2 shows the voltammograms recorded with samples prepared with two Na_3RhCl_6 concentrations and several t_{SD} values, compared to those recorded with a carefully polished Rh disk electrode (inset). The fact that the voltammograms in Fig. 2 are somewhat stretched along the x-axis may be due to the porous nature of the Rh-Ni foam electrodes [40]. The intensity of the peaks due to hydrogen adsorption/desorption onto/from Rh [39] increased with t_{SD}, for each [Na_3RhCl_6], and with [Na_3RhCl_6], for each t_{SD} value. The Rh surface area per unit volume of Ni foam (a_{Rh}) was calculated as:

$$a_{Rh} = \frac{Q_f A_d}{V_f Q_d} \quad (4)$$

where Q_f and Q_d are the H desorption charges for the foam and disk, respectively, V_f is the foam volume, and A_d is the disk geometric area, assumed identical to the true one. Since Q_f and Q_d slightly declined during successive cycles (see inset), the second cycle was considered for all samples. The a_{Rh} values were further used to calculate the Rh surface area per unit Rh mass (a^m_{Rh}) as:

$$a^m_{Rh} = \frac{a_{Rh}}{L_{Rh}} \quad (5)$$

In Fig. 3, a_{Rh} and a^m_{Rh} are plotted as a function of L_{Rh}. Clearly, a_{Rh} increased sublinearly with L_{Rh} and, therefore, a^m_{Rh} decreased with it. At all Rh loadings, the deposits

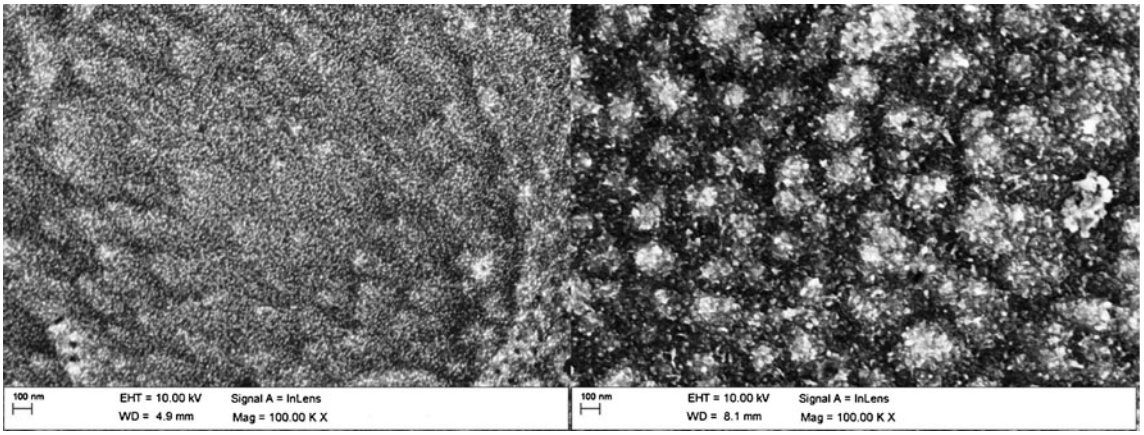

Fig. 1 SEM images of Rh-Ni foam samples prepared with $[Na_3RhCl_6]=1\times10^{-3}$ M (*left*, $L_{Rh}=2.09$ mg cm^{-3}) or $[Na_3RhCl_6]=4\times10^{-4}$ M (*right*, $L_{Rh}=2.36$ mg cm^{-3})

formed in the more concentrated solution had higher surface areas. The upper a^m_{Rh} values, 50 to 60 m^2 g^{-1}, were significantly higher than those obtained in previous studies on noble metal deposition onto Ni foams [19, 25, 26, 37].

Reduction of Nitrate Ions

Nitrate reduction was studied, by cyclic voltammetry, in deaerated solutions containing 1 M NaOH and 0.1 M $NaNO_3$; under these conditions, typical of alkaline waste solutions like those resulting from nuclear plants [41], Rh-Ni electrodes were stable towards corrosion in this basic medium, whereas some corrosion should be expected in acid media. Figure 4a shows the voltammograms (scan towards negative potential only) recorded with Rh-Ni electrodes with five different loadings. All curves show cathodic peaks in the range −0.77 to −0.825 V, followed by a current decrease and a further exponential increase at $E<-0.9$ V. The current measured with unmodified Ni foam electrodes was virtually zero in the potential region of the peak. According to previous studies [29–33], the current peak was due to nitrate reduction, the current decrease to suppression of the former process by adsorbed hydrogen and nitrate reduction intermediates, and the exponential current increase to both reduction of N-containing species and

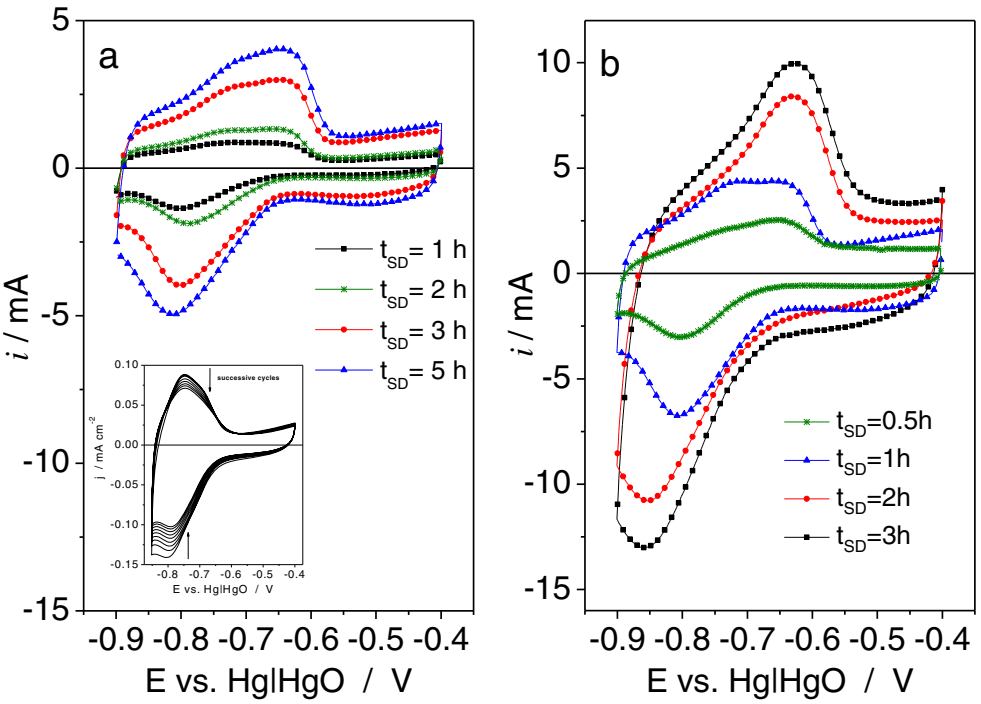

Fig. 2 Cyclic voltammograms recorded with Rh-Ni electrodes (0.0425 cm^3 volume) in 1 M KOH. The electrodes were prepared by immersing Ni foams in 1 M NaCl solutions (pH 2.0) containing either 4×10^{-4} M (*left*) or 10^{-3} M (*right*) Na_3RhCl_6, for different time durations indicated on the figure. Scan rate 50 mV s^{-1}. The *inset* in **a** shows successive cyclic voltammograms recorded with a Rh disk electrode (0.0078 cm^2 geometric area), under the same conditions

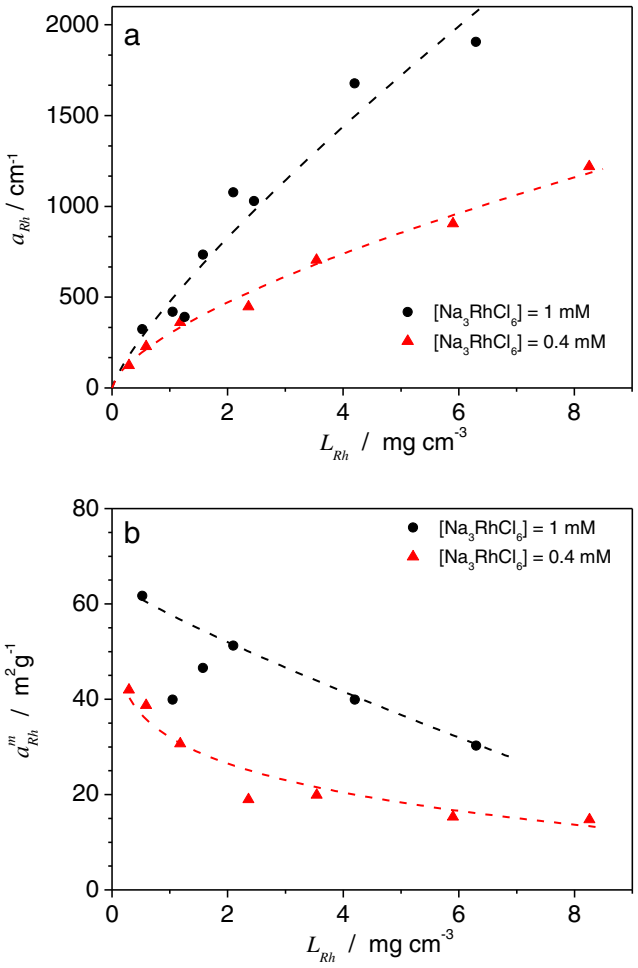

Fig. 3 Dependence of the Rh surface area (**a**) and Rh surface area per unit Rh mass (**b**) on the Rh loading of Rh-Ni samples. The Na_3RhCl_6 concentration in the solutions used in the electrode preparation is indicated on the figures. The *dashed lines* are only an aid for the eye

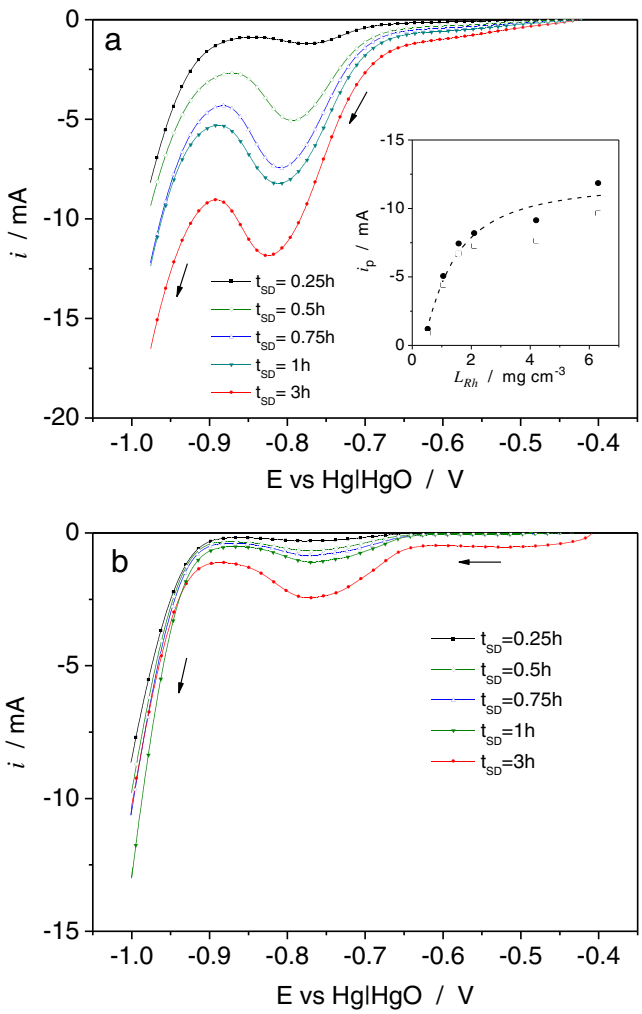

Fig. 4 Cyclic voltammograms recorded with R-Ni foam electrodes (prepared in 10^{-3} M Na_3RhCl_6 solutions, with the deposition times indicated on the figure; 0.0425 cm^3 volume) in **a** 1 M NaOH, 0.1 M $NaNO_3$ or **b** 1 M NaOH. Scan rate 10 mV s^{-1}. The *inset* in **a** shows the dependence of the peak current on Rh loading, without (*full symbols*) and with (*empty symbols*) correction for the contribution of H adsorption

H_2 evolution. Figure 4b, in agreement with Fig. 2, shows that cathodic peaks, due to H adsorption, were recorded around E=−0.8 V with the same electrodes also in the absence of nitrate ions. Therefore, the peaks seen in Fig. 4a were not purely due to nitrate reduction; for each Rh loading, the ratio of the intensities of the nitrate reduction and H adsorption peaks was around 5.

The inset in Fig. 4a shows that the peak current (i_p) increased with the Rh loading in a sublinear way (data are shown both without and with correction for the contribution of H adsorption). The peak current density, referred to the Rh true surface area, computed as

$$j_p = \frac{i_p}{V_f a_{Rh}} = \frac{i_p}{A_{Rh}} \quad (6)$$

where A_{Rh} denotes the total Rh surface area of the sample, was above 2 mA cm^{-2} (1.6 mA cm^{-2}, if corrected for H adsorption) for L_{Rh} of the order of 1 mg cm^{-3}, and decreased to ca. 1 mA cm^{-2} as L_{Rh} increased (Brylev et al. [30] reported values between 0.5 and 0.8 mA cm^{-2}). The decrease of j_p with increasing L_{Rh} was coherent with previous papers (see [33] and references therein) reporting that nitrate reduction was partially controlled by mass transport which, using a quiescent electrolyte, might not be fully efficient in the inner parts of the foam, especially at high current, i.e., at high loading.

Figure 5 compares the linear voltammograms recorded with a Rh-Ni foam electrode in 0.1 M solutions of either NO_3^- or NO_2^- ions and shows that the reduction of the latter occurred with a slightly less negative onset potential and an almost 10 times higher i_p. This suggests that, in electrolyses of nitrate solutions with Rh-Ni

foam electrodes, nitrite ions produced in reaction (7) were likely to be further reduced, e.g., in reaction (8)

$$NO_3^- + H_2O + 2e^- \rightarrow NO_2^- + 2OH^- \quad (7)$$

$$NO_2^- + 5H_2O + 6e^- \rightarrow NH_3 + 7OH^- \quad (8)$$

In order to analyze the composition of the mixture of products obtained by reducing nitrates with Rh-Ni foam and pristine Ni foam electrodes, and to assess the stability of their performance, potentiostatic electrolyses were carried out in 1 M NaOH, 0.1 M $NaNO_3$ solutions. The current measured in electrolyses carried out at the peak potential declined fairly rapidly; thus, a more negative potential (E= −1.20 V) was selected. Taking into account the Ohmic drop iR_Ω, where R_Ω is the uncompensated Ohmic resistance, such a potential corresponded initially to ca. −0.95 V, and became more negative as i declined. Figure 6 shows how the current measured with two Rh-Ni foam electrodes, with two different loadings, and a Ni foam electrode changed in the initial period of time during which a 500-C charge was transferred. The Rh-Ni foam electrodes had a much higher activity than pristine Ni foams, and this activity was higher for the higher L_{Rh} value. The performance of all electrodes slowly declined as the reduction charge increased. A total reduction charge of 2,000 C was transferred in each electrolysis. Trends similar to those shown in Fig. 6, with progressively lower currents, were observed during successive periods of time necessary to transfer 500 C each, up to a reduction charge of 2,000 C (not shown).

The consumption of nitrate and the production of both nitrite and ammonia were measured by ion chromatography,

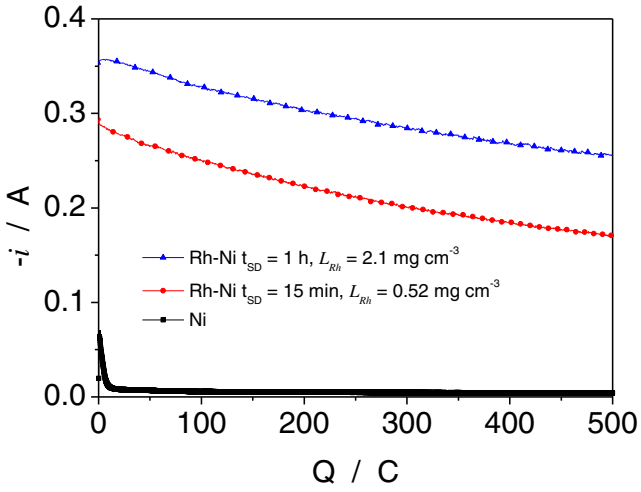

Fig. 6 Chronoamperometric curves recorded with Ni foam or Rh-Ni foam electrodes as indicated on the figure (0.17 cm^3 volume) in 1 M NaOH, 0.1 M $NaNO_3$ solutions, at E=−1.20 V

for different reduction charges. Figure 7 summarizes the results of these analyses, for electrolyses carried out with Rh-Ni foam electrodes. Clearly, ammonia was the main product, and nitrite accounted only for a few percent of the reduced nitrate. NH_2OH was looked for, but not detected. The overall current efficiencies ($\bar{\varepsilon}$) for the nitrate reduction to nitrite and ammonia, calculated from the analytical data, are reported in Table 1. The efficiency was higher for the higher L_{Rh} value and decreased as the reduction charge increased. Although the selected cathode potential might cause some hydrogen evolution, the current efficiency for nitrate reduction was quite high. In the initial period

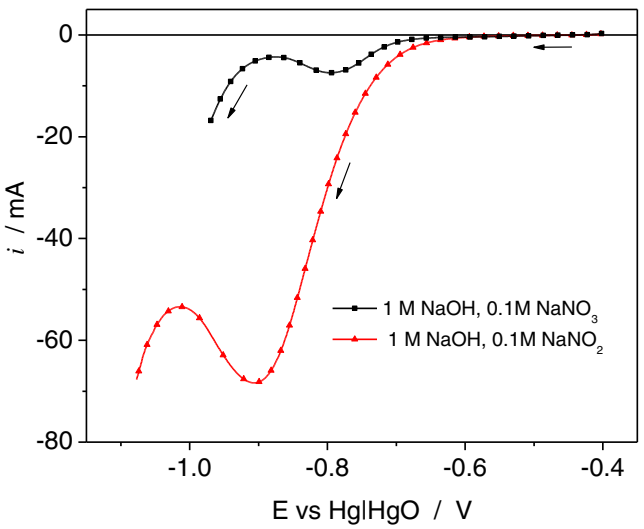

Fig. 5 Comparison of cyclic voltammograms recorded with a Rh-Ni foam electrode (0.0425 cm^3 volume, L_{Rh}=1.6 mg cm^{-3}) in the solutions indicated on the figure. Scan rate 10 mV s^{-1}. Ohmic drop was corrected

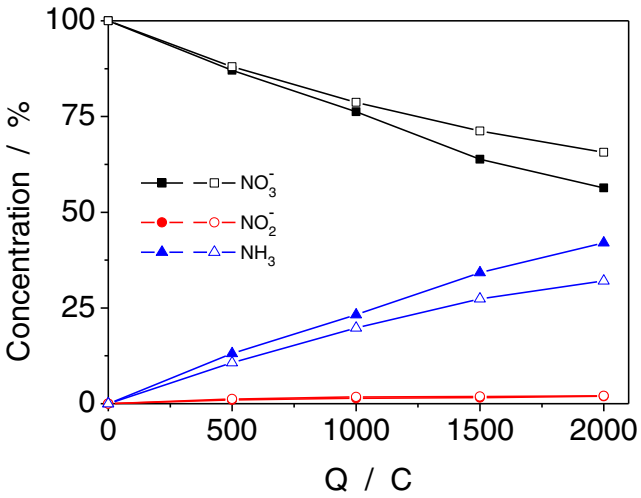

Fig. 7 Dependence of the concentrations of nitrate, nitrite, and ammonia (referred to the initial nitrate concentration) on the reduction charge. The electrolyses were performed with Rh-Ni foam electrodes (0.17 cm^3 volume; *full symbols* t_{SD}=1 h, L_{Rh}=2.1 mg cm^{-3}; *empty symbols* t_{SD}=15 min, L_{Rh}=0.52 mg cm^{-3}) in 1 M NaOH, 0.1 M $NaNO_3$ solutions, at a potential E=−1.20 V

Table 1 Current efficiencies and mass activities measured in electrolyses carried out with Rh-Ni foam electrodes in 1 M NaOH, 0.1 M $NaNO_3$, as a function of the reduction charge. E=−1.20 V

Reduction charge/C	Rh-Ni L_{Rh}=2.1 mg cm^{-3}		Rh-Ni L_{Rh}=0.52 mg cm^{-3}	
	Average current efficiency $\bar{\varepsilon}$/%	Average mass activity $\overline{i_{Rh}}$/A g^{-1}	Average current efficiency $\bar{\varepsilon}$/%	Average mass activity $\overline{i_{Rh}}$/A g^{-1}
0 to 500	100	850	84	2,100
500 to 1,000	90	490	77	1,250
1,000 to 1,500	88	360	71	850
1,500 to 2,000	81	250	62	510

necessary to transfer 500 C, it was essentially 100 % with L_{Rh}=2.1 mg cm^{-3} and 85 % with L_{Rh}=0.52 mg cm^{-3}. One cannot exclude that some hydrogen formed and rapidly reacted with NO_2^- to form NH_3 [34]. The decreasing $\bar{\varepsilon}$ values measured by prolonging the electrolyses were caused, at least in part, by the progressive drift of the true cathode potential towards more negative values, as the reduction current declined. The current efficiency obtained with Ni cathodes, under comparable electrolysis conditions, was 13 % [27]. The quantitative conversion of nitrate to nitrite and ammonia showed that formation of the most desirable reduction product, N_2, was negligible. Both the high current efficiency and the nature of the reduction products suggest that, for the Rh-Ni cathodes, reduction reactions took place almost exclusively on Rh.

Table 1 also reports the average mass activities ($\overline{i_{Rh}}$) calculated by taking into account average reduction currents ($\bar{i}$), average current efficiencies, and Rh loadings, i.e.,

$$\overline{i_{Rh}} = \frac{\overline{i\,\varepsilon}}{V_f L_{Rh}} \tag{9}$$

During the initial period, mass activities were 850 and 2,100 A g^{-1} for the higher and lower loadings, respectively. They progressively declined as the reduction charge increased but remained quite high. Comparing these values with mass activities reported in the literature is not easy because, to the best of our knowledge, no data obtained with the same approach are available. However, Brylev et al. [30] computed mass activity as the ratio between the current measured in cyclic voltammetry at −0.85 V vs. Ag/AgCl (which is close to the peak current) and the Rh mass, finding values are in the range of 50 to 175 A g^{-1}. In our experiments, the peak current per unit Rh mass ($i_{p,Rh}$) is defined as:

$$i_{p,Rh} = \frac{i_p}{V_f L_{Rh}} \tag{10}$$

$i_{p,Rh}$ was higher than 100 A g^{-1} at low Rh loading around 1 mg cm^{-3}, and then declined for increasing L_{Rh} values to become 50 A g^{-1} for L_{Rh}>5 mg cm^{-3}.

With the aim of assessing to what extent the current decrease shown in Fig. 6 was due to the progressive consumption of nitrate ions, the reduction current i_{calc} that should have been measured, after transferring different charges, was calculated by assuming the current and [NO_3^-] to be proportional and the initial intrinsic activity of the electrodes to remain unchanged, as

$$i_{calc} = i_0 \frac{[NO_3^-]_Q}{[NO_3^-]_0} \tag{11}$$

where i_0 denotes the initial current, [NO_3^-]$_0$ the initial nitrate concentration, and [NO_3^-]$_Q$ the nitrate concentration after the transfer of a charge Q. The i_{calc} values are compared to the experimental current values in Table 2 which shows that the progressive depletion of the solution was not sufficient to explain the experimentally observed i-Q dependence. Taking into account the efficiency values reported in Table 1, the trends for both electrodes would be somewhat more pronounced than shown in Table 2. Since measurements of the H desorption charge showed that the Rh surface area had not decreased after nitrate reduction, it must be concluded that the current decrease was partly due to poisoning of the electrodes, which was more significant for the lower L_{Rh} and became stronger as the electrolyses progressed. According to Duca et al. [34], poisoning should be due to adsorbed NH_x species. Besides poisoning, among the possible causes for the current decline, the formation of some H_2 bubbles within the pores of the foam might be of some importance in the later part of the electrolyses. Nevertheless, the deactivation of Rh-Ni foam electrodes was less marked than that of other materials.

The effect of mass transport on the nitrate reduction current was tested using a cell which allowed to impose an electrolyte flow through the Rh-modified Ni foam electrode pores. Figure 8a shows the dependence of the current on the cell voltage (ΔV_{cell}), measured with a quiescent solution or at the maximum flow rate allowed by the experimental setup. By scanning the cell voltage, both the anodic and the cathodic interfacial potential differences were modified. However, the variations were expected to be small at the Pt

Table 2 Dependence on reduction charge of current (i), residual nitrate concentration, and current calculated by assuming current and $[NO_3^-]$ to be proportional and the initial intrinsic activity of the electrodes to remain unchanged (i_{calc}). Electrolyses were carried out with Rh-Ni foam electrodes in 1 M NaOH, 0.1 M $NaNO_3$. E=−1.20 V

Reduction charge/C	Rh-Ni L_{Rh}=2.1 mg cm^{-3}			Rh-Ni L_{Rh}=0.52 mg cm^{-3}		
	i/A	$[NO_3^-]$/M	i_{calc}/A	i/A	$[NO_3^-]$/M	i_{calc}/A
0	−0.36	0.1	−0.36	−0.29	0.1	−0.29
500	−0.26	0.087	−0.31	−0.17	0.088	−0.25
1,000	−0.17	0.076	−0.27	−0.11	0.079	−0.23
1,500	−0.125	0.064	−0.23	−0.09	0.071	−0.21
2,000	−0.09	0.056	−0.20	−0.06	0.066	−0.19

counter electrode immersed in the $[Fe(CN)_6]^{3-}/[Fe(CN)_6]^{4-}$ solution because this redox couple is kinetically fast and both species were present at rather high concentrations. Independent experiments allowed to assess that a 20 mA $[Fe(CN)_6]^{4-}$ oxidation current let the Pt potential shift by less than 50 mV. Nitrate reduction peaks were visible in both i-ΔV_{cell} curves in Fig. 8a, located at −1.25 and −1.27 V, for the quiescent and the flowing solution, respectively. These positions agreed with the peak potentials shown in Fig. 3a, taking into account that the potential of the Pt electrode in contact with the $[Fe(CN)_6]^{3-}/[Fe(CN)_6]^{4-}$ solution was ca. 0.38 V vs. Hg|HgO. Figure 8a shows a significant, though not very large, effect of forced mass transfer.

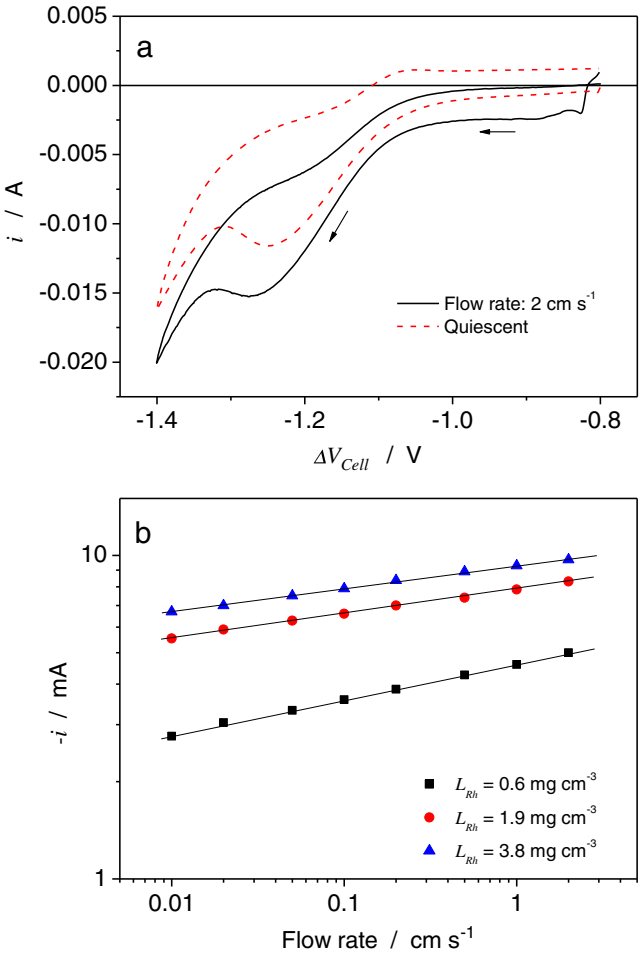

Fig. 8 **a** Comparison of the i-ΔV_{cell} curves obtained with a Rh-Ni foam electrode (L_{Rh}=3.8 mg cm^{-3}) in a 1-M KOH, 0.1-M $NaNO_3$ solution, either quiescent or flowing at 2 cm s^{-1}. ΔV_{cell} was varied at 10 mV s^{-1}. **b** Dependence of the current measured at ΔV_{cell}=−1.20 V on the electrolyte flow rate; the Rh loadings are indicated on the figure

To further characterize the effect of the flow rate on the nitrate reduction current, a constant ΔV_{cell}=−1.20 V was imposed to the cell, the flow rate was stepped from 0 to variable non-zero values and back, every 30 s, and the current was measured. At variance with the experiments in which ΔV_{cell} varied in time, this constant-cell-voltage approach allowed to measure the nitrate reduction current without a significant contribution by the H adsorption current which was significant under potentiodynamic conditions but became negligible at the steady state. Figure 8b shows the dependence of the quasi-stationary current measured at the end of each step on the flow rate, for three different Rh loadings. The current increased with L_{Rh}, as expected, but in a sublinear way (compare with Fig. 3). The slopes of the bilogarithmic plots were always quite low and progressively decreased from 0.11 to 0.075 and to 0.071 as L_{Rh} increased from 0.62 to 1.92 and to 3.84 mg cm^{-3}. The fact that these slopes were much lower than 1 showed that the nitrate reduction process was far from pure mass transfer control [2].

Conclusions

The spontaneous deposition onto Ni foams of Rh nanoparticles, with surface area per unit Rh mass higher than 50 m^2 g^{-1}, was used as a method to prepare effective catalysts for the cathodic reduction of nitrates. These catalysts have several appealing features that may be of interest in the treatment of polluted effluents: (1) they are easy to prepare; (2) their electrochemically active surface/volume ratio is large; (3) due to the low Rh loading, their overall cost may be reasonably low; (4) their activity is comparable with that of the best catalysts described in the literature; (5) their resistance to poisoning is quite good; and (6) the geometry of the Ni foams is appropriate for their use under forced electrolyte flow conditions. Like most catalysts based

on noble metals, the Rh-modified Ni foam electrodes reduced nitrates mainly to ammonia. N_2 production was negligible under all the explored conditions.

Acknowledgments The authors gratefully acknowledge the financial support of the Italian Ministry for Economic Development (MSE), MSE-CNR Agreement on National Electrical System.

References

1. R.E. Sioda, Electrochim. Acta. **13**, 1559 (1968)
2. R. Alkire, B. Gracon, J. Electrochem. Soc. **122**, 1594 (1975)
3. R.J. Marshall, F.C. Walsh, Surf. Technol. **24**, 45 (1985)
4. J.M. Marracino, F. Coeuret, S. Langlois, Electrochim. Acta **32**, 1303 (1987)
5. J. González–Garcia, V. Montiel, A. Aldaz, J.A. Conesa, J.R. Pérez, G. Codina, Ind. Eng. Chem. Res. **37**, 4501 (1998)
6. R. Menini, Y.M. Henuset, J. Fournier, J. Appl. Electrochem. **35**, 625 (2005)
7. M. Matlosz, J. Newman, J. Electrochem. Soc. **133**, 1850 (1986)
8. J.M. Friedrich, C. Ponce–de–León, G.W. Reade, F.C. Walsh, Electroanal. Chem. **561**, 203 (2004)
9. B.K. Ferreira, Miner. Process. Ext. Metall. Rev. **29**, 330 (2008)
10. I. Sirés, E. Brillas, Environ. Int. **40**, 212 (2012)
11. C. Carlesi Jara, D. Fino, V. Specchia, G. Saracco, P. Spinelli, Appl. Catal. B Environ. **70**, 479 (2007)
12. J. Muff, C.D. Andersen, R. Erichsen, E.G. Soegaard, Electrochim. Acta **54**, 2062 (2009)
13. J.M. Skowronski, A. Wazny, J. Sol. Struct. Electrochem. **9**, 890 (2005)
14. W. Yang, S. Yang, W. Sun, G. Sun, Q. Xin, J. Power Sources **160**, 1420 (2006)
15. W. Yang, S. Yang, W. Sun, G. Sun, Q. Xin, Electrochim. Acta **52**, 9 (2006)
16. F. Bidault, D.J.L. Brett, P.H. Middleton, N. Abson, N.P. Brandon, Int. J. Hydrogen Energy **34**, 6799 (2009)
17. F. Bidault, D.J.L. Brett, P.H. Middleton, N. Abson, N.P. Brandon, Int. J. Hydrogen Energy **35**, 1783 (2010)
18. Y.-L. Wang, Y.-Q. Zhao, C.-L. Xu, D.-D. Zhao, M.-W. Xu, Z.-X. Su, H.-L. Li, J. Power Sources **195**, 6496 (2010)
19. Y. Yamauchi, M. Kumatsu, A. Takai, R. Sebata, M. Sawada, T. Momma, M. Fuziwara, T. Osaka, K. Kuroda, Electrochim. Acta **53**, 604 (2007)
20. D. Cao, Y. Guo, G. Wang, R. Miao, Y. Liu, Int. J. Hydrogen Energy **35**, 807 (2010)
21. Y. Cheng, Y. Liu, D. Cao, G. Wang, Y. Gao, J. Power Sources **196**, 3124 (2011)
22. J.M. Skowronski, A. Czerwinski, T. Rozmanowski, Z. Rogulski, P. Krawczyk, Electrochim. Acta **52**, 5677 (2007)
23. B. Yang, G. Yu, D. Shuai, Chemosphere **67**, 1361 (2007)
24. B. Yang, G. Yu, J. Huang, Environ. Sci. Technol. **41**, 7503 (2007)
25. E. Verlato, S. Cattarin, N. Comisso, A. Gambirasi, M. Musiani, L. Vázquez–Gómez, Electrocatalysis **3**, 48 (2012)
26. S. Fiameni, I. Herraiz–Cardona, M. Musiani, V. Pérez–Herranz, L. Vázquez–Gómez, E. Verlato, Int. J. Hydrogen Energy **37**, 10507 (2012)
27. H. Li, D.H. Robertson, J.Q. Chambers, D.T. Hobbs, J. Electrochem. Soc. **135**, 1154 (1988)
28. H. Li, D.H. Robertson, J.Q. Chambers, D.T. Hobbs, J. Appl. Electrochem. **18**, 454 (1988)
29. G.E. Dima, A.C.A. de Vooys, M.T.M. Koper, J. Electroanal. Chem. **554–555**, 15 (2003)
30. O. Brylev, M. Sarrazin, D. Bélanger, L. Roué, Appl. Catal., B **64**, 243 (2006)
31. O. Brylev, M. Sarrazin, L. Roué, D. Bélanger, Electrochim. Acta **52**, 6237 (2007)
32. P.M. Tucker, M.J. Waite, B.E. Hayden, J. Appl. Electrochem. **34**, 781 (2007)
33. V. Rosca, M. Duca, M.T. de Groot, M.T.M. Koper, Chem. Rev. **109**, 2209 (2009)
34. M. Duca, B. van der Klugt, M.A. Hasnat, M. Machida, M.T.M. Koper, J. Catal. **275**, 61 (2010)
35. N. Comisso, S. Cattarin, S. Fiameni, R. Gerbasi, L. Mattarozzi, M. Musiani, L. Vázquez- Gómez, E. Verlato, Electrochem. Comm. **25**, 91 (2012)
36. L. Mattarozzi, S. Cattarin, N. Comisso, P. Guerriero, M. Musiani, L. Vázquez-Gómez, E. Verlato, Electrochim. Acta **89**, 488 (2013)
37. S. Cimino, L. Lisi, G. Mancino, M. Musiani, L. Vázquez–Gómez, E. Verlato, Int. J. Hydrogen Energy **37**, 17040 (2012)
38. E. Benguerel, G.P. Demopoulos, G.B. Harris, Hydrometallurgy **40**, 135 (1996)
39. R. Woods, Chemisorption at electrodes: hydrogen and oxygen on noble metals and their alloys, in *Electroanalytical Chemistry*, ed. by A.J. Bard, vol. 9 (Marcel Dekker, New York, 1976), p. 1
40. B. Conway, in *Impedance Spectroscopy*, ed. by E. Barsoukov, J.R. Macdonal (Wiley, Hoboken, 2005), pp. 469
41. J.D. Genders, D. Hartsough, D.T. Hobbs, J. Appl. Electrochem. **26**, 1 (1988)